Environmental Science and Ecotechnology 17 (2024) 100303

Contents lists available at ScienceDirect

Environmental Science and Ecotechnology

journal homepage: www.journals.elsevier.com/environmental-science-and-ecotechnology/

Original Research

Selective butyric acid production from CO_2 and its upgrade to butanol in microbial electrosynthesis cells

Meritxell Romans-Casas [a], Laura Feliu-Paradeda [b], Michele Tedesco [c], Hubertus V.M. Hamelers [c], Lluis Bañeras [b], M. Dolors Balaguer [a], Sebastià Puig [a], Paolo Dessì [a, *]

[a] LEQUiA, Institute of the Environment, University of Girona. Campus Montilivi, Carrer Maria Aurèlia Capmany 69, E-17003, Girona, Spain
[b] Molecular Microbial Ecology Group, Institute of Aquatic Ecology, University of Girona, Maria Aurèlia Capmany 40, 17003, Girona, Spain
[c] Wetsus, European Centre of Excellence for Sustainable Water Technology, Oostergoweg 9, 8911, MA, Leeuwarden, the Netherlands

ARTICLE INFO

Article history:
Received 3 March 2023
Received in revised form
16 July 2023
Accepted 22 July 2023

Keywords:
Biocathode
Bioelectrochemical system
Chain elongation
Hydrogen partial pressure
Megasphaera

ABSTRACT

Microbial electrosynthesis (MES) is a promising carbon utilization technology, but the low-value products (i.e., acetate or methane) and the high electric power demand hinder its industrial adoption. In this study, electrically efficient MES cells with a low ohmic resistance of 15.7 mΩ m^2 were operated galvanostatically in fed-batch mode, alternating periods of high CO_2 and H_2 availability. This promoted acetic acid and ethanol production, ultimately triggering selective (78% on a carbon basis) butyric acid production via chain elongation. An average production rate of 14.5 g m^{-2} d^{-1} was obtained at an applied current of 1.0 or 1.5 mA cm^{-2}, being *Megasphaera* sp. the key chain elongating player. Inoculating a second cell with the catholyte containing the enriched community resulted in butyric acid production at the same rate as the previous cell, but the lag phase was reduced by 82%. Furthermore, interrupting the CO_2 feeding and setting a constant pH_2 of 1.7–1.8 atm in the cathode compartment triggered solventogenic butanol production at a pH below 4.8. The efficient cell design resulted in average cell voltages of 2.6–2.8 V and a remarkably low electric energy requirement of 34.6 kWh_{el} kg^{-1} of butyric acid produced, despite coulombic efficiencies being restricted to 45% due to the cross-over of O_2 and H_2 through the membrane. In conclusion, this study revealed the optimal operating conditions to achieve energy-efficient butyric acid production from CO_2 and suggested a strategy to further upgrade it to valuable butanol.

1. Introduction

The development of efficient carbon capture and utilization (CCU) technologies with low power demand is compulsory to achieve the Sustainable Development Goal (SDG) 13 on climate action, while also avoiding negative impacts on other SDGs [1]. Among these technologies, microbial electrosynthesis (MES) has emerged as a promising approach for the electricity-driven CO_2 reduction to biofuels and platform chemicals by chemo-lithoautotrophic organisms [2,3]. To date, acetate and methane have been selectively produced from CO_2 and electricity in MES cells using a mixed culture of microorganisms as inoculum. Remarkable coulombic efficiencies approaching 100% have been reported for both products [4,5]. However, their low market value (<€0.7 kg^{-1}) compared to their production costs challenges the industrial adoption. Thus, recent studies focus on producing more valuable compounds, such as ethanol and middle-chain fatty acids.

Ethanol can be produced from acetic acid by solventogenic microorganisms mainly belonging to the genus *Clostridium* [6,7]. Ethanol production in MES cells has often been reported upon acetic acid accumulation. Romans-Casas et al. [8] achieved the highest ethanol production rate of nearly 11 g m^{-2} d^{-1}) after acetic acid accumulated to 6 g L^{-1} in the catholyte by operating an H-type cell under high hydrogen partial pressure (pH_2 > 3 atm) and low pH (<4.5). The produced ethanol can be extracted, purified and commercialized, or further converted into higher-value products, such as butyric acid, via chain elongation pathways [9].

* Corresponding author.
E-mail address: paolo.dessi@udg.edu (P. Dessì).

https://doi.org/10.1016/j.ese.2023.100303

A thorough metagenomic survey confirmed the genetic potential of MES microbiomes to produce elongated (C_4 and C_6) carboxylic acids and alcohols from CO_2 [10]. Chain elongation is carried out by anaerobic microorganisms, such as some *Clostridium*, *Megasphaera*, and *Caproiciproducens* strains that convert a C_n to a C_{n+2} carboxylic acid using ethanol or lactate as electron donors. This occurs via reverse β-oxidation or fatty acid biosynthesis pathways [9]. Thus, in the first chain elongation cycle, acetic acid is elongated to butyric acid, a chemical with a market value of circa €1.8 kg^{-1} that finds application in the pharmaceutical, farming, perfume, and chemical sectors [11]. Butyric acid production from CO_2 in MES cells was first reported by Ganigué et al. [12] and later in several studies [13–16]. However, butyric acid was always produced in mixtures with other carboxylic acids without exceeding 50% selectivity, making the follow-up downstream step difficult. Various techniques can separate carboxylic acids, including liquid-liquid extraction, membrane separation, adsorption, and electrodialysis [17]. However, regardless of the technique applied, the selective extraction of butyric acid from a mixture of carboxylic acids remains a challenge. Therefore, improving the selectivity of the production stage is crucial to achieving cost-effectiveness.

Butanol production was occasionally reported along with butyric acid in MES cells [10,12,18,19]. Butanol has great industrial importance as a *drop-in* biofuel compatible with the current gasoline infrastructures [20] and also finds application in the pharmaceutical and chemical industries as a precursor to acrylate and methacrylate [21]. Selective extraction and purification of butanol from mixtures is simpler than doing the same for butyric acid, as it can be accomplished through distillation or by innovative, more energy-efficient methods like pervaporation [22]. Rovira-Alsina et al. [23] developed a thermodynamic model to predict the best conditions to trigger the production of elongated carboxylic acids and alcohols and reported that butanol production should be favoured at low pH and high pH_2. Although thermodynamics is not the only factor affecting production in biological systems, setting up operational conditions enhancing the thermodynamics of a specific reaction is an effective starting point to optimize production rates and specificity experimentally.

Besides the conversion efficiency, selectivity, and market value of the final product, the techno-economic feasibility of MES widely depends on the electric efficiency of the cells. Most of the studies on MES have been performed in inefficient H-type cells, characterised by high ohmic resistance and requiring as high as 7 V to deliver current densities of 3–4 mA cm^{-2} [8]. In addition to high operational costs, technologies with a high power demand have been demonstrated to have a collateral effect on population health, water scarcity, and mineral/metal resources on a large scale [1]. Therefore, compact, scalable electrochemical cells with low ohmic resistance are imperative to reduce overpotentials, minimizing the electric power input for product synthesis. Efficient, scalable, flat-plate cells with a minimum distance between the cathode and anode electrodes (i.e., low- and zero-gap configurations) have been designed to perform electrochemical CO_2 reduction [24] and recently proposed for bioelectrochemical systems [25].

Previous studies revealed the potential of MES for the conversion of CO_2 to valuable butyric acid and butanol [10,18]. However, increasing product selectivity to facilitate downstream processing while minimizing the electric energy expenses is imperative to bring this technology towards commercialization. This study aimed to develop a strategy to achieve high-selectivity butyric acid production from CO_2 in electrically efficient low-gap (with a 2-mm distance between the electrodes) MES cells and unravel the combination of operation conditions (pH_2, pCO_2, and pH) that trigger its further conversion to butanol.

2. Materials and methods

2.1. Electrochemical cell set-up

The experiments were conducted in two commercial electrochemical cells (MicroFlowCell, ElectroCell Europe, Denmark): EC-1 and EC-2 (Fig. S1). The cells were equipped with a dimensionally stable anode (DSA-O_2) and a carbon felt cathode electrode of 10 cm^2 projected area each, separated by a reinforced cation exchange membrane (CEM, Nafion N324, US). The volume of the cathode and anode chambers was 4 and 3 mL, respectively. The cathode chamber was sealed to prevent gas exchange with the atmosphere and promote the accumulation of H_2, whereas the anode chamber was open to prevent oxygen accumulation. Recirculation lines were built using glass bottles as buffer tanks, marprene tubes, and a peristaltic pump (Watson Marlow 205U, UK). The tubes were equipped with sampling ports for liquid (both cathodic and anodic chamber) and gas (only cathodic chamber). An Ag/AgCl reference electrode (+0.197 V vs. SHE, model RE-5B, BASI, UK) was inserted in the recirculation line at about 10 cm from the cathode since the cell design did not allow installation near the cathode.

2.2. Electrochemical cell operation

The cathode chamber of EC-1 was inoculated with a mixed culture dominated by *Clostridium* sp., shown to produce ethanol in H-type MES cells [8]. The inoculum was mixed with a mineral medium at a 1:10 v/v ratio. The medium used as both anolyte and catholyte was described by Romans Casas et al. [8]. A total medium volume of 80 mL was recirculated through a buffer tank at a rate of 5.2 mL min^{-1} resulting in an up-flow velocity of 2.5 m h^{-1} in the cathode chamber. This configuration resulted in a headspace of 76 mL in the buffer tank (Fig. S1). EC-1 was connected to a potentiostat (BioLogic, Model VSP, France) in a three-electrode configuration and operated for 152 days at ambient temperature (25–32 °C) under galvanostatic conditions. Cathode potential and cell voltage were continuously monitored. The applied current was increased stepwise from 0.3 to 3.0 mA cm^{-2}, as indicated in Fig. 1. EC-1 was operated in fed-batch mode, where the catholyte was sparged with CO_2 (99.9 %, Air Liquide, Spain) for at least 3 min thrice a week. After sparging, an initial partial pressure (pCO_2) of either 1.3 atm (on days 0–14) or 1.5 atm (from days 16 onwards) was set at the beginning of each fed-batch cycle by closing the gas outlet of the cathode and regulating the pressure valve of the gas cylinder to the desired pressure. Besides this, between days 44 and 126, additional CO_2 was added twice per week to avoid CO_2 depletion by

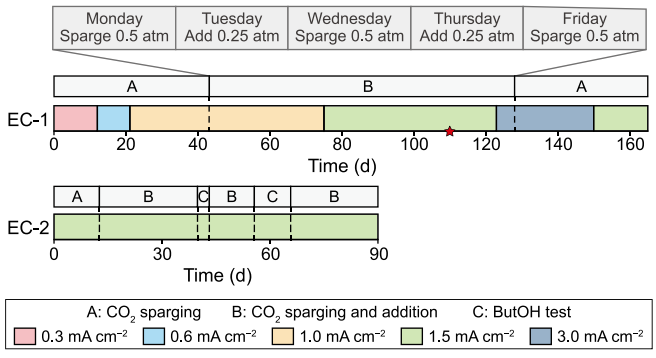

Fig. 1. Operation timeline of EC-1 and EC-2. The weekly CO_2 feeding schedule is indicated in the box. The red star indicates the day that 10% of EC-1 catholyte was withdrawn to inoculate EC-2.

the microbial community (Fig. 1). It was done by adding CO_2 from the gas cylinder until the pressure of the cathode was increased by 0.25 atm without sparging. Sodium 2-bromoethanesulphonate (Na-BES, 1 g L^{-1}) was added upon methane detection in the catholyte headspace (on days 28, 82, and 112).

EC-2 was inoculated with the EC-1 catholyte (1:10 v/v ratio) after 110 days of experimentation and operated under the same conditions but setting a current density of 1.5 mA cm^{-2} and a pCO_2 of 1.5 atm from the beginning. EC-2 was operated in a two-electrode configuration where only the cell voltage was continuously monitored, whereas the cathode potential was measured on sampling days with a multimeter (Lendher IMY64). Na-BES was added on days 2 and 44 to prevent methanogenesis. Besides the three weekly sparging and addition to 0.5 atm, extra CO_2 (0.25 atm) was supplied twice per week from day 16 onwards (Fig. 1). Butanol production tests (ButOH tests) were performed on days 44 and 56 by stopping the CO_2 supply and letting the hydrogen partial pressure (pH_2) increase to 1.7–1.8 atm, which was then kept constant using a pressure-release valve. After the test, the CO_2 supply was restored.

2.3. Chemical and electrochemical analyses

Liquid samples (3 mL) of both catholyte and anolyte and a gas sample (5 mL) from the cathode were collected thrice weekly before CO_2 sparging. The liquid withdrawn was replaced with CO_2-sparged fresh medium to maintain constant volumes. The optical density (OD, 600 nm) of the catholyte and anolyte was measured with a spectrophotometer DR3900 (Hach, Germany). The conductivity and pH of liquid samples were assessed by the respective measuring instruments (EC-meter basic 30+ and pH meter Basic 20+, Crison Instruments, Spain). Gas pressure in the cathode headspace was measured by using a digital pressure sensor (differential pressure gauge, Testo 512, Spain). The concentration of carboxylic acids and alcohols in the catholyte and anolyte was measured in pre-filtered (0.2 μm) samples with a gas chromatograph (GC 7890 A, Agilent Technologies, USA) equipped with a DB-FFAP column and a flame ionization detector (FID). Gas composition was monitored by a GC (Micro GC 490, Agilent Technologies, USA) equipped with a thermal conductivity detector (TCD) and two columns: a CP-Molesieve 5A with helium as the carrier gas for CH_4, CO, H_2, O_2, and N_2 analysis, and a CP-Poraplot U with argon as the carrier gas for CO_2 analysis. Details on both liquid and gas analysis are published elsewhere [8].

Electrochemical impedance spectroscopy (EIS) was performed before cell inoculation in two-electrode configurations to estimate the ohmic drop (R_Ω) of the cell. A potential of 0 V vs. open circuit voltage (OCV) and a sinusoidal wave of 10 mA in the frequency range from 10 MHz to 100 kHz with 10 points per logarithmic decade was applied. Cyclic voltammetry (CV) was performed on the same day in a three-electrode configuration by sweeping the potential from 0 to −0.5 V vs. SHE at 1 mV s^{-1} scan rate for three replicate cycles. The CV results were corrected against the uncompensated resistance of 0.115 Ω between cathode and reference, estimated by three-electrode EIS.

2.4. Calculations

The production rates were calculated as the amount of product synthesised in the time unit (sum of product detected in the catholyte and anolyte) normalized to either the cathode projected surface (10 cm^2) or the catholyte volume (80 mL). Product selectivity was calculated as the percentage of carbon recovered in a specific product in relation to the total carbon recovered in carboxylic acid or alcohol. The electric energy requirement (E) in kWh kg^{-1} was calculated as in equation (1), where P is the electric power consumed in the time period Δt, ΔCi_{cat} and ΔCi_{an} are the increase in the concentration of the product i in the catholyte and anolyte, respectively, and V is the electrolyte volume.

$$E = \frac{P \times \Delta t}{(\Delta Ci_{cat} + \Delta Ci_{an}) \times V} \quad (1)$$

The coulombic efficiency (CE) was calculated as in equation (2), where F is the Faraday constant (96485.33 C mol^{-1}), M_i is the moles of the product i, Δe_i is the moles of electrons required per mol of product formed by CO_2 reduction, and $\int Idt$ is the electric charge supplied along the period considered.

$$CE\ (\%) = \frac{F \times \sum_i M_i \times \Delta e_i}{\int Idt} \times 100 \quad (2)$$

2.5. Microbial community analysis

Catholyte samples (5–8 mL) were collected before each change in the applied current density (EC-1) and before and after butanol production tests (in EC-2) for analysis of the suspended microbial community. The catholyte removed was replaced with the same amount of CO_2 sparged, freshly prepared medium. Suspended cell samples were centrifuged at 4400 rpm for 30 min at 4 °C, supernatants were discarded, and pellets were stored at −20 °C until DNA extraction. A sample of carbon felt (1 cm^2) was collected from EC-2 at the end of the experiment and stored at −20 °C to analyse the attached microbial community.

DNA was extracted using the FastDNA® SPIN kit for Soils (MP Biomedicals, USA) following the manufacturer's instructions and quantified using a Qubit® 2.0 Fluorometer with the QubitTM dsDNA HS Assay Kit (Thermo Fisher Scientific, US). The hypervariable V4 region of the 16S rRNA gene was amplified by polymerase chain reaction (PCR) using the 515F-806R primer pair [26]. High-throughput sequencing was conducted at the RTSF core facilities at Michigan State University USA (https://rtsf.natsci.msu.edu/) through Illumina PE 250 MiSeq platform. Raw sequences were analysed using DADA2 [27]. Sequences were sorted, quality-filtered, trimmed to a consistent length, dereplicated, denoised, and merged to eliminate sequencing errors, to finally obtain a sequence table with the inferred amplicon sequence variant (ASVs). The taxonomy of each ASV sequence was assigned using the SILVA 138.1 database (https://www.arb-silva.de/). Data were treated using the phyloseq R package to analyse the relative abundance at the genus level [27]. All sequences obtained in this study have been submitted to the GenBank database under the SRA accession number PRJNA926809.

3. Results and discussion

3.1. Bioelectrochemical CO_2 conversion to butyric acid

After inoculating EC-1, microbial growth was detected from the first days of operation, as suggested by the linear OD increase from 0.027 to 0.161 by day 21 (Fig. 2). Despite this, no organic products were synthesised from CO_2 on days 0–12 at an applied current of 0.3 mA cm^{-2}. Acetic acid production was detected immediately after increasing the applied current density to 0.6 mA cm^{-2} (Fig. 2), with a linear production rate of 10.0 g m^{-2} d^{-1} (0.13 g L^{-1} d^{-1}) on days 12–19 (Table 1), before slowing down on days 19–21. Acetic acid production resumed at a constant rate of 5.5 g m^{-2} d^{-1} after increasing the applied current to 1.0 mA cm^{-2} until day 54. The

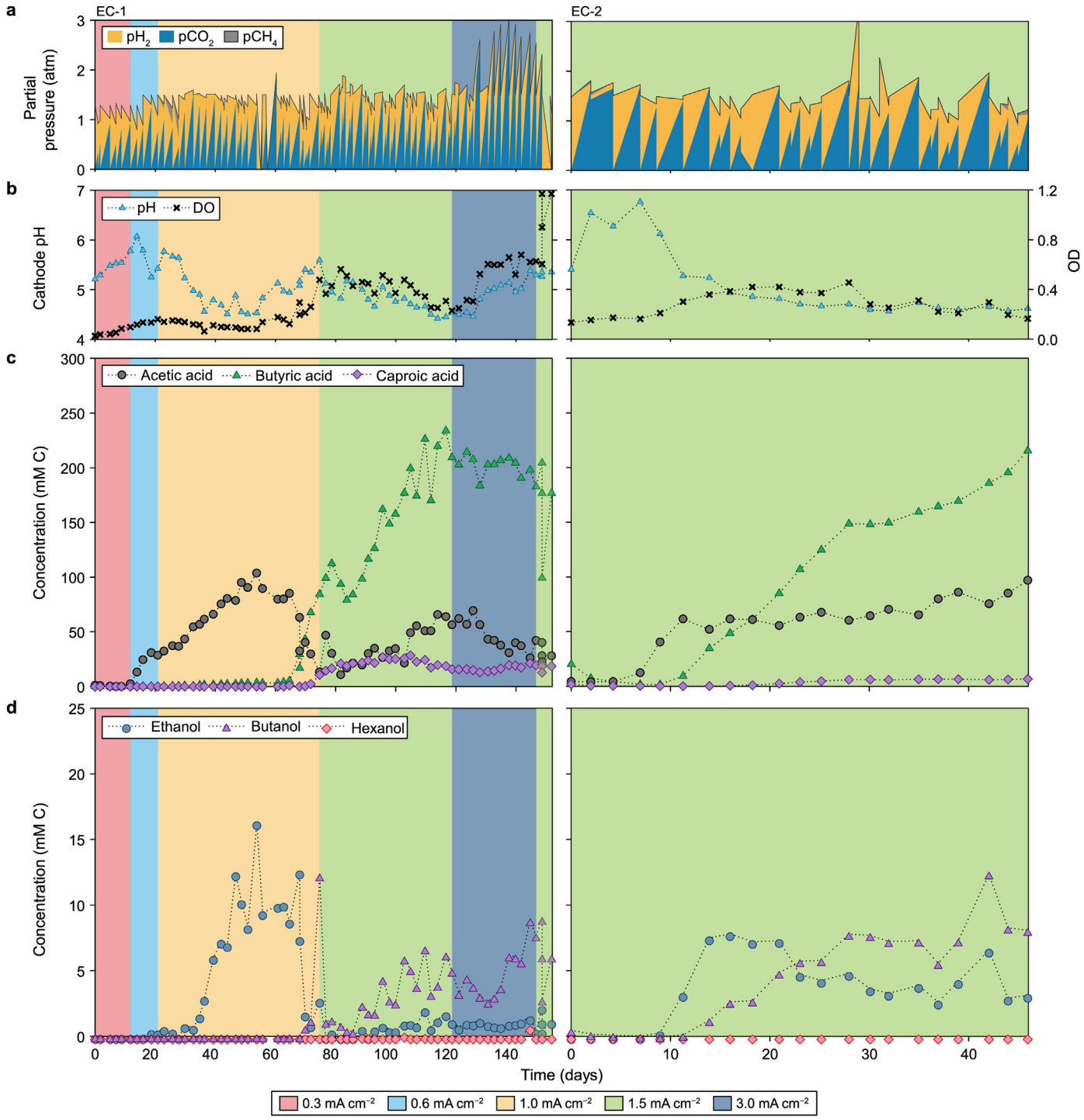

Fig. 2. Partial pressures (**a**), pH and OD (**b**), and carboxylic acid (**c**) and alcohol (**d**) production profiles (sum of cathode and anode concentrations) in EC-1 (left) and EC-2 (right) at the different current densities applied.

highest concentration obtained at the cathode was 2.6 g L^{-1} (Fig. S2). Concomitantly, the pH naturally decreased from 5.8 (day 23) to 4.5 (day 54) and eventually led to the inhibition of acetic acid production (Fig. 2).

Acetic acid accumulation and the pH decrease triggered the onset of solventogenesis [28]. Ethanol was produced concomitantly with acetic acid from day 30 onwards, although its concentration remained low (<20 mM C). On day 63, acetic acid and ethanol concentrations decreased, and longer C-chains compounds (mainly butyric acid) were formed. This shift was due to the onset of chain-elongating pathways [29]. After increasing the current to 1.5 mA cm^{-2} on day 75, ethanol was only detected in low amounts (<2 mM C), suggesting its rapid consumption by chain-elongating microorganisms. Butyric acid concentrations increased, although with some fluctuations, likely due to the increased availability of H_2 in the reactor. The observed fluctuations in butyric acid concentration were presumably due to competitive reactions such as solventogenic butanol production and further elongation to caproic

acid (Fig. 2). Additionally, a portion of butyric acid was likely oxidized due to O_2 diffusion from the anodic to the cathodic chamber, an ongoing challenge in MES [30]. Despite these factors, a linear ($R^2 > 0.95$) butyric acid production with a rate of 14.5 g m^{-2} d^{-1} (0.17 g L^{-1} d^{-1}) was observed on days 65–79 (Table 1). This rate was independent of the applied current density of 1.0 mA cm^{-2} (on days 65–75) or 1.5 mA cm^{-2} (on days 75–79). These results suggest that butyric acid synthesis was limited by the ethanol production rate, despite the increased availability of reducing equivalents at higher currents. Butyric acid was produced until day 117, reaching a total of 234 mM C. The highest butyric acid concentration in the catholyte was 3.2 g L^{-1} (Fig. S2).

Caproic acid production started after day 70 when butyric acid concentration at the cathode was near 1 g L^{-1}. It was produced at a rate of 2.0 g m^{-2} d^{-1} on days 77–82, up to a maximum of 24 mM C on day 91, before declining until day 126. No net carboxylic acid or alcohol production was achieved after increasing the applied current density to 3.0 mA cm^{-2} on day 126, despite the increased H_2 production and the pH rise from 4.5 to 5.3. This can be attributed to a progressive biofilm detachment caused by the increased H_2 production [31], as suggested by the increase in OD (Fig. 2). Furthermore, doubling the applied current likely intensified O_2 diffusion from the anode, causing an increased product consumption by aerobic organisms.

During cell operation, the gas pressure at the cathode followed a cyclic trend, where pCO_2 decreased from the initial set value of 1.3–1.5 atm (feast conditions) towards negative pressures (famine conditions) due to consumption by bacteria for their metabolism and product synthesis. Concomitantly, pH_2 increased over time proportionally to the current applied (Fig. 2). The average pH_2 at the end of each batch cycle was 0.73 ± 0.20, 0.87 ± 0.27, 1.02 ± 0.34, 1.33 ± 0.26, and 2.52 ± 0.38 atm at an applied current of 0.3, 0.6, 1.0, 1.5, and 3.0 mA cm^{-2}, respectively. The alternate periods with high and low H_2 availability (and the opposite CO_2 trend) favoured the solventogenic and acetogenic pathways, respectively, ultimately leading to butyric acid production via chain elongation with over 70% selectivity (Table 1).

To further assess the replicability of the process, a second cell (EC-2) was inoculated with 8 mL (10%) of catholyte from EC-1 and operated under similar conditions, excluding the current density, which was set to 1.5 mA cm^{-2} from the beginning. Acetic acid production began on day 7, and its concentration rapidly increased to 62 mM C (day 12) and then slowed down, reaching 97 mM C by day 46. Ethanol concentration remained below 8 mM C, as it was consumed for butyric acid production by chain elongation. Butyric acid production was observed from day 12 (Fig. 2). The lag phase was 82% lower than in EC-1, confirming that enriched cultures of chain-elongating microorganisms can start up MES cells in a relatively short time. Butyric acid was produced linearly on days 14–28, with an average rate of 14.2 g m^{-2} d^{-1}, similar to the rate obtained in EC-1 (Table 1). During this period, it was produced with a remarkable 78% selectivity (on a carbon basis), well above those achieved in previous studies [16,18,32]. From day 28 onwards, the production rates declined, likely due to the increased butyric acid concentrations in the catholyte (around 2.3 g L^{-1}) (Fig. S2) in combination with low pH (<4.8). Nevertheless, butyric acid was still produced until day 44, reaching 196 mM C. Butanol and caproic acid were detected from day 14 onwards and reached 8.3 and 6.4 mM C, respectively. The concentration of caproic acid was considerably lower than those typically achieved from acetic acid and ethanol in fermentation bioreactors [9]. It appears that the further elongation of butyric acid to caproic acid was impeded by the low ethanol:acetic acid ratio in the catholyte resulting in the slow ethanol production kinetics in MES cells [32], despite the relatively high pH_2 achieved in this study.

Table 1
Operation conditions and average performance parameters of the EC-1 and EC-2 cells during the periods of linear ($R^2 > 0.95$) production.

Cell	Period (d)	Product	Operational conditions						Performance parameters				
			Current applied (mA cm^{-2})	Cell voltage (V)	Cathode potential (V vs. SHE[a])	pH range	pH_2 (atm)	OD[b] (AU)	Production rate (g m^{-2} d^{-1})	Production rate (mg L^{-1} d^{-1})	Power requirement (kWh kg^{-1})	CE[c] (%)	Selectivity (%)
EC-1	12–19	Acetic acid	0.6	2.40	−0.55	5.4–6.1	0.91	0.12	10.0	125.4	34.4	25.5	95.8
	21–54	Acetic acid	1.0	2.57	−0.51	4.5–5.8	1.14	0.11	5.5	68.8	111.1	7.2	59.2
	65–79	Butyric acid	1.0	2.58	−0.50	4.9–5.6	0.85	0.28	14.5	181.5	34.6	45.3	74.2
	86–105	Butyric acid	1.5	2.75	−0.52	4.7–5.2	1.36	0.44	10.0	124.4	94.3	17.7	60.7
	77–82	Caproic acid	1.5	2.75	−0.51	4.8–5.1	1.08	0.45	2.0	25.2	434.8	4.6	23.3
EC-2	7–11	Acetic acid	1.5	2.67	−0.42	5.3–6.8	1.34	0.22	27.3	340.9	34.5	27.6	82.6
	14–28	Butyric acid	1.5	2.66	−0.47	4.7–5.3	1.38	0.38	14.2	177.4	65.4	24.6	77.6
	18–28	Caproic acid	1.5	2.67	−0.46	4.7–4.9	1.50	0.41	0.8	10.1	1111.1	1.7	4.6
	46–51	Butanol	1.5	2.68	−0.40	4.6–4.7	1.80	0.17	2.2	27.0	416.7	5.6	27.9
	67–72	Butanol	1.5	2.70	−0.43	4.7–4.9	1.74	0.27	1.4	17.8	625.0	3.8	18.3

[a] Standard hydrogen electrode.
[b] Optical density in absorbance units.
[c] Coulombic efficiency.

3.2. Butyric acid upgrade to butanol

In EC-1, butanol production fluctuated on days 88–125, with a concentration above 2 g L^{-1} of butyric acid and pH below 5. The fluctuation was due to the intermittent high pH_2 and pCO_2 conditions. The butanol production peaks were obtained in concomitance with high pH_2 (1.5–1.7 atm) and low pCO_2 (<0.05 atm) (Fig. 2), whereas it was consumed in periods with high carbon availability. A highly positive Pearson correlation (T-score: 6.742, *p*-value <0.05) between butanol selectivity and pH_2, as well as a positive Pearson correlation (T-score: 3.903, *p*-value < 0.05) between butanol production rate and pH_2, were observed in this phase (Fig. S3).

To further investigate this phenomenon, the CO_2 supply was interrupted for one week in EC-2 on days 46–56 (ButOH test 1, Fig. 3) when the butyric acid concentration at the cathode was around 3 g L^{-1} (Fig. S2), pH was 4.6, and a stable pH_2 of 1.78 ± 0.04 atm was maintained in the cell through a pressure release valve. Butanol was linearly produced for five days with an average production rate and selectivity of 2.2 g m^{-2} d^{-1} and 28%, respectively, before stopping due to a pH increase to 4.9. Similarly, Ganigué et al. [12] and Srikanth et al. [18] reported butanol production rates of 2–3 g m^{-2} d^{-1} at pH values of 4.5–4.6, though with substantially lower selectivity than in this study. This suggests that maintaining a pH below the pK_A of butyric acid (i.e., 4.82) is imperative to trigger butanol production. At pH 4.6, nearly 70% of the butyric was in the undissociated form, which is the most toxic form for the microorganisms, triggering the defensive solventogenic mechanism [33]. Therefore, high butyric acid accumulation, low pH, lack of inorganic carbon, and high pH_2 (at least 1.5–1.7 atm) are simultaneously needed to trigger butanol production from butyric acid via solventogenesis, as previously reported for ethanol production from acetic acid [7].

As expected, acetogenesis ceased during the test due to the lack of CO_2, but acetic acid was progressively converted to butyric acid, suggesting that chain elongating pathways were still active in the absence of CO_2. This is an expected result, as acetogenesis is the only CO_2-requiring metabolic reaction in the system. Ethanol concentration also increased during CO_2 depletion, confirming that solventogenic pathways are favoured under those conditions when the corresponding carboxylic acid is present. From day 50 onwards, the increasing pH resulted in a depletion of alcohol concentrations, which became more evident after resuming the CO_2 feeding on day 56, suggesting the reversibility of the bioreaction [7]. Repeating the test on days 67–79 (ButOH test 2, Fig. 3) confirmed the same trends, although the production rate was 35% lower due to the slightly higher initial pH (4.73 vs. 4.61).

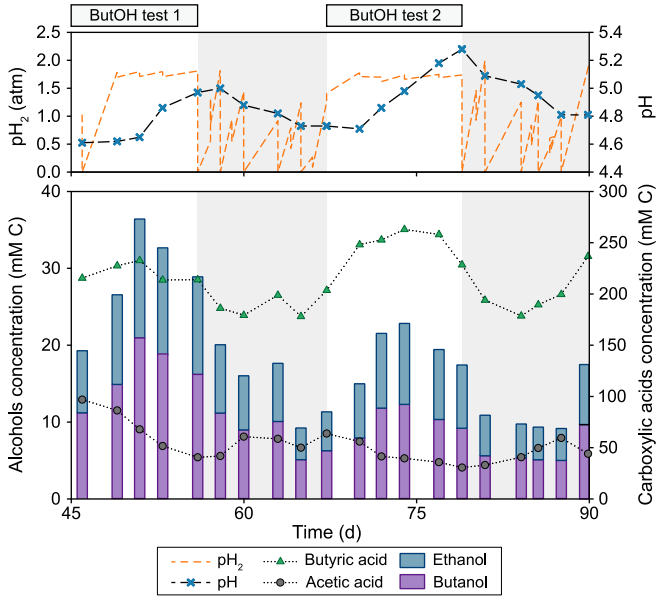

Fig. 3. H_2 accumulation tests (ButOH test 1 and ButOH test 2) performed in EC-2. The white area represents the period where the CO_2 supply was stopped and pH_2 accumulated to 1.78 ± 0.04 atm. The grey area represents the recovering period where CO_2 was supplied again.

3.3. Microbial community analysis

The suspended community of EC-1, originally dominated by species belonging to the genus *Clostridium*, radically changed within the first 12 days of operation at an applied current of 0.3 mA cm^{-2} (Fig. 4). During this period, the relative abundance of *Clostridium* sp. dropped. Accordingly, neither carboxylic acids nor alcohols were produced at such low current density (Fig. 2). *Desulfovibrio* sp., an electrotrophic microorganism capable of catalysing H_2 production at the cathode, was detected on day 12 with a relative abundance of 7%, suggesting that H_2-mediated acetogenesis was taking place [34]. A meta-analysis of MES microbiomes has shown that *Desulfovibrio* is commonly found as the syntrophic partner of acetogenic microorganisms in biocathodes [35]. Increasing the current from 0.3 to 0.6 mA cm^{-2} resulted in an increased relative abundance of acetogenic microorganisms identified as *Sporomusa* sp. (from 1% to 10%) and *Acetobacterium* sp. (from 2% to 5%), with the resulting onset of acetic acid production (Fig. 2). *Sporomusa* sp. has a lower H_2 threshold than most acetogenic microorganisms [36], allowing these organisms to perform acetogenesis through the Wood-Ljungdahl pathway at low applied potential or, in this case, at low applied current.

Further increasing the current to 1 mA cm^{-2} resulted in the revival of *Clostridium* sp. (most likely *Clostridium ljungdahlii*) and *Eubacterium* sp., which were the dominant acetogens in the inoculum, at the expense of *Sporomusa* (<1%), probably due to their faster kinetics for H_2 consumption [36]. Since the cathode potential remained fairly constant at the increasing current density applied (Fig. S4), this result suggested that the availability of reducing equivalents was the main driving force in selecting the acetogenic communities in the E-cells.

In EC-1, after 75 days of operation, *Megasphaera* sp. was detected

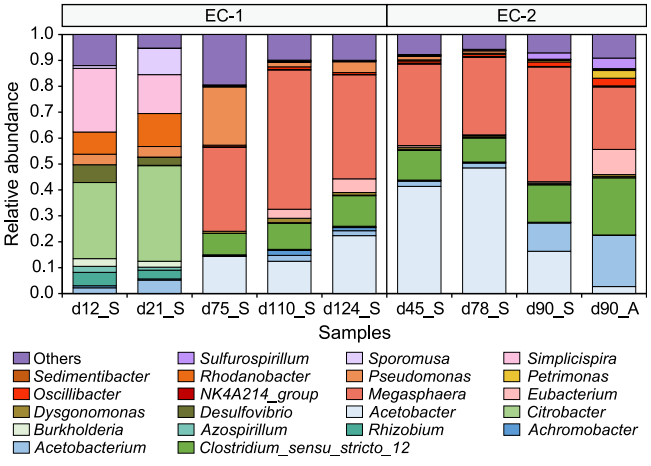

Fig. 4. Genus-level community composition of EC-1 and EC-2 at different time points. ASVs found in a relative abundance <1% were grouped and graphed as Others. S and A stand for suspended and attached community, respectively.

at a relative abundance of 32%, which increased to 54% on day 111. *Megasphaera* has been shown to perform chain elongation from various sugars and lactic acid [9,37], and it was suggested to use ethanol as the electron donor in MES cells to form butyric acid [16]. *Megasphaera* was the most abundant genus in EC-2, with relative abundances between 30% and 44%, and contributed by 24% to the attached community by the end of the experiment (Fig. 4). Such a high relative abundance indicates its key role in butyric acid production in the two cells. Butanol production tests did not substantially affect the composition of the microbial community. Therefore, it can be hypothesized that the shift from acidogenesis to solventogenesis was due to metabolic shifts rather than species substitution.

Current densities of 1.0 mA cm^{-2} and above had the collateral effect of increasing O_2 production at the anode, likely resulting in its faster diffusion of O_2 through the membrane towards the cathode. This was confirmed by the increased relative abundance of facultative or strictly aerobic microorganisms acting as oxygen scavengers [16,38]. In particular, *Acetobacter* sp. reached 22% of sequence reads in EC-1 after increasing the current density to 3.0 mA cm^{-2}. Interestingly, in EC-2, the relative abundance of *Acetobacter* sp. among the attached community was remarkably lower than in the bulk community (Fig. 4). This suggests that the scavengers were effectively shielding the cathodic community from oxygen intrusion, protecting the anaerobic members of the community at the expense of the CEs (Table 1). Overall, the key species found in the attached and suspended communities were similar, although the relative abundances were different, as previously reported [39].

3.4. Perspectives and challenges

Fed-batch operation with alternating periods of high pCO_2 and pH_2 was a suitable strategy to target high-selectivity butyric acid from CO_2 in MES cells. The E-cell was designed to maximise electric efficiency with only a 2-mm distance between the cathode and the anode and a high A_{cat}/V_{cat} of 250 m^2 m^{-3} for microbial adhesion. This resulted in an ohmic resistance of 15.7 mΩ m^2, estimated by EIS analysis (Fig. S4). To our knowledge, a lower ohmic resistance (2.4 mΩ m^2) has been reported only in a methanogenic zero-gap MES flow cell equipped with membrane-electrode assembly and solid anodic electrolyte [40]. This allowed us to achieve an electric power requirement of 34.6 kWh kg^{-1} butyric acid, 2-fold lower than the 64.3 kWh kg^{-1} reported in the literature [13].

As confirmed by CV analysis (Fig. S4), the H_2 onset potential was around −0.5 V, higher than in previous studies performed under galvanostatic conditions [14,41], suggesting a low overpotential for the cathodic hydrogen evolution reaction (HER). Interestingly, increasing applied current density had only a marginal effect on the cathode potential (Fig. S4), suggesting that H_2 production can be sustained at relatively high current densities without significantly increasing the overpotential. Conversely, the anode potential increased significantly with the current applied (from 1.52 V at −0.3 mA cm^{-2} to 2.96 V at −3.0 mA cm^{-2}). Hence, the anodic reaction was the main contributor to the overall cell voltage, which can be reduced by mitigating the pH split between anode and cathode and considering less demanding anodic reactions, such as oxidation of organics [42].

Although the process may not be competitive with the current electricity prices, it should be considered that the cost of renewable energy (mostly solar and wind power) is expected to drop to somewhere between €10 MWh^{-1} and €50 MWh^{-1} by 2050 [43]. Assuming an electricity price of €30 MWh^{-1}, a production cost of around €1 kg^{-1} can be achieved, which would then require additional expenses for extraction and purification, typically accounting for 30–40% of the production cost [44]. The power consumption can be theoretically reduced to as low as 7.5 kWh kg^{-1} when assuming the minimum cell voltage of 1.23 V for water splitting and 100% CE. However, a more realistic voltage of 1.8–2.0 V, as achieved in state-of-art electrolysers [45], would produce an electric power requirement of 10–15 kWh kg^{-1}, potentially making the process competitive with chemical synthesis. Further conversion of the produced butyric acid to butanol, a promising green alternative to traditional fuels [46], will further improve the economics of the process. However, production rates, selectivity, and titer must be improved. This can be accomplished by implementing a controlled system that maintains the required pH (<4.8) and pH_2 (>1.7 atm) following butyric acid accumulation.

Employing compact and modular cells with minimum distance between the electrodes, connected in a multi-stack configuration, represents the most efficient approach to scaling up electrochemical systems, such as MES [47]. However, despite the considerable improvements in electric efficiency, minimizing the distance between electrodes can increase the exposure of the cathodic community to O_2. Cation exchange membranes cannot completely circumvent O_2 diffusion to the cathode, hampering the activity of strictly anaerobic members of the microbial community and/or causing product consumption by microaerophilic microorganisms [30]. Additionally, if not immediately utilized by the microbial community, the H_2 produced at the cathode can permeate towards the anode and escape into the atmosphere. This issue is particularly relevant when the cathodic chamber is maintained under pressure. In this study, it was experimentally measured that 4.6 μmol h^{-1} of H_2 (2.5% of the total produced at 10 mA cm^{-2} applied current) were lost through the membrane at a pH_2 of only 1.12 atm. Considering that the cells reached pH_2 values up to 3 atm, this percentage was inevitably higher, particularly during operation at 1.5 and 3 mA cm^{-2} applied current. The same phenomenon was observed for CO_2, which was shown to permeate through the membrane at a rate of 22 mmol h^{-1} when the pCO_2 was around 1.5 atm. This issue could potentially be solved by employing low-gas permeability membranes. However, to the best of the authors' knowledge, such membranes are yet to be developed and implemented. It is essential to address this problem in the near future and find a solution, as higher current densities are required to scale up MES cells.

4. Conclusion

This study shows that fed-batch operation with alternating periods of high pCO_2 and pH_2 is suitable for promoting butyric acid production from CO_2 in MES cells. A microbial population dominated by *Megasphaera* sp. achieved 78% selectivity, the highest reported so far for butyric acid, at an applied current density of 1.5 mA cm^{-2}. The enriched cathodic community can act as inoculum to obtain butyric acid production in successive cells with reduced start-up time. An efficient cell design with low ohmic resistance helped to reduce the electric power requirement to 34.6 kWh kg^{-1} butyric acid. The produced butyric acid can be further converted to valuable butanol by ceasing the CO_2 supply and maintaining high pH_2 (>1.7 atm) and low pH (<4.8).

CRediT author contribution statement

M. Romans-Casas: Conceptualization, Data Curation, Investigation, Writing - Original Draft. **L. Feliu-Paradeda:** Data Curation, Writing - Reviewing & Editing. **M. Tedesco:** Writing - Reviewing & Editing. **H.V.M. Hamelers:** Writing - Reviewing & Editing. **L. Bañeras:** Writing - Reviewing & Editing. **M.D. Balaguer:** Conceptualization, Writing - Reviewing & Editing, Supervision. **S. Puig:**

Conceptualization, Funding Acquisition, Supervision, Writing - Reviewing & Editing. **P. Dessì:** Conceptualization, Data Curation, Investigation, Writing - Original Draft. All authors have approved the final version of the manuscript.

Declaration of competing interest

The authors declare that they have no known competing financial interests or personal relationships that could have appeared to influence the work reported in this paper.

Acknowledgements

This research was carried out in the project "PANGEA — Process intensificAtioN for bioelectroCO2 recyclinG into carbon-nEutrAl products) funded by the Spanish Ministry of Innovation and Science (ref. PID2021-126240OB-I00). PD is supported by the European Union's Horizon 2020 research and innovation programme under the Marie Skłodowska-Curie grant agreement, project ATMESPHERE, No 101029266. MR-C is grateful for the support of the Spanish Government (FPU20/01362). S.P. is a Serra Hunter Fellow (UdG-AG-575) and acknowledges the funding from the ICREA Academia award. LF-P is grateful for the Research Training grant from the Catalan Government (2021 FISDU 00132). LEQUIA and EcoAqua have been recognized by the Catalan Government (Ref 2021 SGR01352 and 2021 SGR01142).

Appendix A. Supplementary data

Supplementary data to this article can be found online at https://doi.org/10.1016/j.ese.2023.100303.

References

[1] I. Ioannou, Á. Galán-Martín, J. Pérez-Ramírez, G. Guillén-Gosálbez, Trade-offs between sustainable development goals in carbon capture and utilisation, Energy Environ. Sci. 16 (2023) 113–124, https://doi.org/10.1039/d2ee01153k.
[2] P. Dessì, L. Rovira-Alsina, C. Sánchez, G.K. Dinesh, W. Tong, P. Chatterjee, M. Tedesco, P. Farràs, H.V.M. Hamelers, S. Puig, Microbial electrosynthesis: towards sustainable biorefineries for production of green chemicals from CO_2 emissions, Biotechnol. Adv. 46 (2021) 107675, https://doi.org/10.1016/j.biotechadv.2020.107675.
[3] B. Bian, S. Bajracharya, J. Xu, D. Pant, P.E. Saikaly, Microbial electrosynthesis from CO_2: challenges, opportunities and perspectives in the context of circular bioeconomy, Bioresour. Technol. 302 (2020) 122863, https://doi.org/10.1016/j.biortech.2020.122863.
[4] L. Jourdin, Y. Lu, V. Flexer, J. Keller, S. Freguia, Biologically induced hydrogen production drives high rate/high efficiency microbial electrosynthesis of acetate from carbon dioxide, Chemelectrochem 3 (2016) 581–591, https://doi.org/10.1002/celc.201500530.
[5] F. Kracke, J.S. Deutzmann, B.S. Jayathilake, S.H. Pang, S. Chandrasekaran, S.E. Baker, A.M. Spormann, Efficient hydrogen delivery for microbial electrosynthesis via 3D-printed cathodes, Front. Microbiol. 12 (2021) 696473, https://doi.org/10.3389/fmicb.2021.696473.
[6] S. Bajracharya, S. Srikanth, G. Mohanakrishna, R. Zacharia, D.P. Strik, D. Pant, Biotransformation of carbon dioxide in bioelectrochemical systems: state of the art and future prospects, J. Power Sources 356 (2017) 256–273, https://doi.org/10.1016/j.jpowsour.2017.04.024.
[7] R. Blasco-Gómez, S. Ramió-Pujol, L. Bañeras, J. Colprim, M.D. Balaguer, S. Puig, Unravelling the factors that influence the bio-electrorecycling of carbon dioxide towards biofuels, Green Chem. 21 (2019) 684–691, https://doi.org/10.1039/c8gc03417f.
[8] M. Romans-Casas, E. Perona-Vico, P. Dessì, L. Bañeras, M.D. Balaguer, S. Puig, Boosting ethanol production rates from carbon dioxide in MES cells under optimal solventogenic conditions, Sci. Total Environ. 856 (2023) 159124, https://doi.org/10.1016/j.scitotenv.2022.159124.
[9] J. Wang, Y. Yin, Biological production of medium-chain carboxylates through chain elongation: an overview, Biotechnol. Adv. 55 (2022) 107882, https://doi.org/10.1016/j.biotechadv.2021.107882.
[10] I. Vassilev, P.A. Hernandez, P. Batlle-Vilanova, S. Freguia, J.O. Krömer, J. Keller, P. Ledezma, B. Virdis, Microbial electrosynthesis of isobutyric, butyric, caproic acids, and corresponding alcohols from carbon dioxide, ACS Sustain. Chem. Eng. 6 (2018) 8485–8493, https://doi.org/10.1021/acssuschemeng.8b00739.
[11] J.C. Wood, J. Grové, E. Marcellin, J.K. Heffernan, S. Hu, Z. Yuan, B. Virdis, Strategies to improve viability of a circular carbon bioeconomy-A techno-economic review of microbial electrosynthesis and gas fermentation, Water Res. 201 (2021) 117306, https://doi.org/10.1016/j.watres.2021.117306.
[12] R. Ganigué, S. Puig, P. Batlle-Vilanova, M.D. Balaguer, J. Colprim, Microbial electrosynthesis of butyrate from carbon dioxide, Chem. Commun. 51 (2015) 3235–3238, https://doi.org/10.1039/c4cc10121a.
[13] L. Jourdin, S.M.T. Raes, C.J.N. Buisman, D.P.B.T.B. Strik, Critical biofilm growth throughout unmodified carbon felts allows continuous bioelectrochemical chain elongation from CO_2 up to caproate at high current density, Front. Energy Res. 6 (2018) 7, https://doi.org/10.3389/fenrg.2018.00007.
[14] L. Jourdin, M. Winkelhorst, B. Rawls, C.J.N. Buisman, D.P.B.T.B. Strik, Enhanced selectivity to butyrate and caproate above acetate in continuous bioelectrochemical chain elongation from CO_2: steering with CO_2 loading rate and hydraulic retention time, Bioresour Technol Rep 7 (2019) 100284, https://doi.org/10.1016/j.biteb.2019.100284.
[15] K. Tahir, W. Miran, J. Jang, A. Shahzad, M. Moztahida, B. Kim, D.S. Lee, A novel MXene-coated biocathode for enhanced microbial electrosynthesis performance, Chem. Eng. J. 381 (2020) 122687, https://doi.org/10.1016/j.cej.2019.122687.
[16] P. Batlle-Vilanova, R. Ganigué, S. Ramió-Pujol, L. Bañeras, G. Jiménez, M. Hidalgo, M.D. Balaguer, J. Colprim, S. Puig, Microbial electrosynthesis of butyrate from carbon dioxide: production and extraction, Bioelectrochemistry 117 (2017) 57–64, https://doi.org/10.1016/j.bioelechem.2017.06.004.
[17] L. Jiang, H. Fu, H.K. Yang, W. Xu, J. Wang, S.-T. Yang, Butyric acid: applications and recent advances in its bioproduction, Biotechnol. Adv. 36 (2018) 2101–2117, https://doi.org/10.1016/j.biotechadv.2018.09.005.
[18] S. Srikanth, D. Singh, K. Vanbroekhoven, D. Pant, M. Kumar, S.K. Puri, S.S.V. Ramakumar, Electro-biocatalytic conversion of carbon dioxide to alcohols using gas diffusion electrode, Bioresour. Technol. 265 (2018) 45–51, https://doi.org/10.1016/j.biortech.2018.02.058.
[19] S. Srikanth, M. Kumar, D. Singh, M.P. Singh, S.K. Puri, S.S.V. Ramakumar, Long-term operation of electro-biocatalytic reactor for carbon dioxide transformation into organic molecules, Bioresour. Technol. 265 (2018) 66–74, https://doi.org/10.1016/j.biortech.2017.12.075.
[20] T. Pinto, X. Flores-Alsina, K.V. Gernaey, H. Junicke, Alone or together? A review on pure and mixed microbial cultures for butanol production, Renew. Sustain. Energy Rev. 147 (2021) 111244, https://doi.org/10.1016/j.rser.2021.111244.
[21] B. Ndaba, I. Chiyanzu, S. Marx, n-Butanol derived from biochemical and chemical routes: a review, Biotechnology Reports 8 (2015) 1–9, https://doi.org/10.1016/j.btre.2015.08.001.
[22] V.S.S.L.P. Talluri, A. Tleuova, S. Hosseini, O. Vopicka, Selective separation of 1-butanol from aqueous solution through pervaporation using PTSMP-silica nano hybrid membrane, Membranes 10 (2020) 55, https://doi.org/10.3390/membranes10040055.
[23] L. Rovira-Alsina, M. Romans-Casas, M.D. Balaguer, S. Puig, Thermodynamic approach to foresee experimental CO_2 reduction to organic compounds, Bioresour. Technol. 354 (2022) 127181, https://doi.org/10.1016/j.biortech.2022.127181.
[24] S. Liang, N. Altaf, L. Huang, Y. Gao, Q. Wang, Electrolytic cell design for electrochemical CO_2 reduction, J. CO2 Util. 35 (2020) 90–105, https://doi.org/10.1016/j.jcou.2019.09.007.
[25] R. Rossi, G. Baek, B.E. Logan, Vapor-fed cathode microbial electrolysis cells with closely spaced electrodes enables greatly improved performance, Environ. Sci. Technol. 56 (2022) 1211–1220, https://doi.org/10.1021/acs.est.1c06769.
[26] J.J. Kozich, S.L. Westcott, N.T. Baxter, S.K. Highlander, P.D. Schloss, Development of a dual-index sequencing strategy and curation pipeline for analyzing amplicon sequence data on the Miseq illumina sequencing platform, Appl. Environ. Microbiol. 79 (2013) 5112–5120, https://doi.org/10.1128/AEM.01043-13.
[27] B.J. Callahan, P.J. McMurdie, M.J. Rosen, A.W. Han, A.J.A. Johnson, S.P. Holmes, DADA2: high-resolution sample inference from Illumina amplicon data, Nat. Methods 13 (2016) 581–583, https://doi.org/10.1038/nmeth.3869.
[28] K. Arslan, B. Bayar, H. Nalakath Abubackar, M.C. Veiga, C. Kennes, Solventogenesis in *Clostridium aceticum* producing high concentrations of ethanol from syngas, Bioresour. Technol. 292 (2019) 121941, https://doi.org/10.1016/j.biortech.2019.121941.
[29] W. de A. Cavalcante, R.C. Leitão, T.A. Gehring, L.T. Angenent, S.T. Santaella, Anaerobic fermentation for n-caproic acid production: a review, Process Biochem. 54 (2017) 106–119, https://doi.org/10.1016/j.procbio.2016.12.024.
[30] M. Abdollahi, S. al Sbei, M.A. Rosenbaum, F. Harnisch, The oxygen dilemma: the challenge of the anode reaction for microbial electrosynthesis from CO_2, Front. Microbiol. 13 (2022) 947550, https://doi.org/10.3389/fmicb.2022.947550.
[31] J. Li, Z. Li, S. Xiao, Q. Fu, H. Kobayashi, L. Zhang, Q. Liao, X. Zhu, Startup cathode potentials determine electron transfer behaviours of biocathodes catalysing CO_2 reduction to CH_4 in microbial electrosynthesis, J. CO2 Util. 35 (2020) 169–175, https://doi.org/10.1016/j.jcou.2019.09.013.
[32] S.M.T. Raes, L. Jourdin, C.J.N. Buisman, D.P.B.T.B. Strik, Continuous long-term bioelectrochemical chain elongation to butyrate, Chemelectrochem 4 (2017) 386–395, https://doi.org/10.1002/celc.201600587.
[33] M. Kumar, K. Gayen, S. Saini, Role of extracellular cues to trigger the metabolic phase shifting from acidogenesis to solventogenesis in *Clostridium acetobutylicum*, Bioresour. Technol. 138 (2013) 55–62, https://doi.org/10.1016/j.biortech.2013.03.159.

[34] E. Perona-Vico, L. Feliu-Paradeda, S. Puig, L. Bañeras, Bacteria coated cathodes as an in-situ hydrogen evolving platform for microbial electrosynthesis, Sci. Rep. 10 (2020) 1−11, https://doi.org/10.1038/s41598-020-76694-y.
[35] S. Mills, P. Dessì, D. Pant, P. Farràs, W.T. Sloan, G. Collins, U.Z. Ijaz, A meta-analysis of acetogenic and methanogenic microbiomes in microbial electrosynthesis, NPJ Biofilms Microbiomes 8 (2022) 73, https://doi.org/10.1038/s41522-022-00337-5.
[36] J. Philips, Extracellular electron uptake by acetogenic bacteria: does H_2 consumption favor the H_2 evolution reaction on a cathode or metallic iron? Front. Microbiol. 10 (2020) 2997, https://doi.org/10.3389/fmicb.2019.02997.
[37] S. Kang, H. Kim, B.S. Jeon, O. Choi, B.I. Sang, Chain elongation process for caproate production using lactate as electron donor in *Megasphaera hexanoica*, Bioresour. Technol. 346 (2022) 126660, https://doi.org/10.1016/j.biortech.2021.126660.
[38] M. Isipato, P. Dessì, C. Sánchez, S. Mills, U.Z. Ijaz, F. Asunis, D. Spiga, G. de Gioannis, M. Mascia, G. Collins, A. Muntoni, P.N.L. Lens, Propionate production by bioelectrochemically-assisted lactate fermentation and simultaneous CO_2 recycling, Front. Microbiol. 11 (2020) 1−16, https://doi.org/10.3389/fmicb.2020.599438.
[39] P. Dessì, C. Sánchez, S. Mills, F.G. Cocco, M. Isipato, U.Z. Ijaz, G. Collins, P.N.L. Lens, Carboxylic acids production and electrosynthetic microbial community evolution under different CO_2 feeding regimens, Bioelectrochemistry 137 (2021) 107686, https://doi.org/10.1016/j.bioelechem.2020.107686.
[40] G. Baek, R. Rossi, P.E. Saikaly, B.E. Logan, High-rate microbial electrosynthesis using a zero-gap flow cell and vapor-fed anode design, Water Res. 219 (2022) 118597, https://doi.org/10.1016/j.watres.2022.118597.
[41] P. Dessì, C. Buenaño-Vargas, S. Martínez-Sosa, S. Mills, A. Trego, U.Z. Ijaz, D. Pant, S. Puig, V. O'Flaherty, P. Farràs, Microbial electrosynthesis of acetate from CO_2 in three-chamber cells with gas diffusion biocathode under moderate saline conditions, Environ. Sci.Ecotechnology 16 (2023) 100261, https://doi.org/10.1016/j.ese.2023.100261.
[42] L. Jourdin, T. Burdyny, Microbial electrosynthesis: where do we go from here? Trends Biotechnol. 39 (2021) 359−369, https://doi.org/10.1016/j.tibtech.2020.10.014.
[43] J.L.L.C.C. Janssen, M. Weeda, R.J. Detz, B. van der Zwaan, Country-specific cost projections for renewable hydrogen production through off-grid electricity systems, Appl. Energy 309 (2022) 118398, https://doi.org/10.1016/j.apenergy.2021.118398.
[44] J. Chun, O. Choi, B.I. Sang, Enhanced extraction of butyric acid under high-pressure CO_2 conditions to integrate chemical catalysis for value-added chemicals and biofuels, Biotechnol. Biofuels 11 (2018) 119, https://doi.org/10.1186/s13068-018-1120-1.
[45] T. Wang, X. Cao, L. Jiao, PEM water electrolysis for hydrogen production: fundamentals, advances, and prospects, Carbon Neutrality 1 (2022) 21, https://doi.org/10.1007/s43979-022-00022-8.
[46] S.I. Meramo-Hurtado, Á. González-Delgado, L. Rehmann, E. Quinones-Bolanos, M. Mehvar, Comparative analysis of biorefinery designs based on acetone-butanol-ethanol fermentation under exergetic, techno-economic, and sensitivity analyses towards a sustainability perspective, J. Clean. Prod. 298 (2021) 126761, https://doi.org/10.1016/j.jclepro.2021.126761.
[47] D.A. Jadhav, A.D. Chendake, V. Vinayak, A. Atabani, M. Ali Abdelkareem, K.J. Chae, Scale-up of the bioelectrochemical system: strategic perspectives and normalization of performance indices, Bioresour. Technol. 363 (2022) 127935, https://doi.org/10.1016/j.biortech.2022.127935.